

COMPACTION OF COPPER NANOPOWDER

S. P. Kiselev

UDC 539.3 + 539.4

The problem of void filling in a copper nanocell under external loading generated by a spherical piston is solved. It is demonstrated by computations that a copper nanocell is an unstable system. Small perturbations generated by piston motion lead to void filling under the action of surface tension and to release of significant amounts of thermal energy. After the voids are filled, the initial crystalline structure of nanoparticles is violated and becomes amorphous. When the nanocell is rapidly compressed, a metastable state with a strongly distorted crystal lattice arises, which transforms to an amorphous state with significant amounts of heat released.

Key words: nanocell, void, copper, molecular dynamics, pressure, temperature, energy.

Introduction. A number of experimental techniques for creating nanostructural coatings by means of compaction of nanopowders by shock waves have been developed [1–3]. These techniques, however, have no reliable theoretical justification. The difficulties in calculating nanopowder compaction are caused by an important role of processes of different scales. The characteristic spatial scales vary from nanometers (diameter of nanoparticles and voids) to centimeters (specimen diameter), and the time scales vary from femtoseconds to microseconds. It is next to impossible to take into account all scales in one computation. The present paper describes nanoscale computations by the method of molecular dynamics [4]. Physical and mechanical processes inherent in compaction of a cell consisting of eight copper nanoparticles subjected to compression by a spherical piston are considered.

Formulation of the Problem. Let us consider the problem of compaction of a characteristic cell under external loading. We assume that nanoparticles in the cell have dense cubic packing, which is loaded by a spherical piston (Fig. 1). The nanocell consists of eight densely packed copper nanoparticles of radius R_p located at the apices of a cube with a rib length l . There are voids at the center of the nanocell and on the side faces of the cube. The volume of the void located on the side face of the cube is half the volume of the void at the cube center.

To calculate the nanocell deformation under the action of a spherical piston, we use the method of molecular dynamics [4]. The motion of copper atoms is described by the Hamilton equations [4]

$$\frac{dp_{a,i}}{dt} = -\frac{\partial H}{\partial x_{a,i}}, \quad \frac{dx_{a,i}}{dt} = \frac{\partial H}{\partial p_{a,i}},$$

$$H = K + \sum_{a=1}^N V_{\text{ext}}(x_{a,i}) + U(x_{a,i}), \quad K = \sum_{a=1}^N \sum_{i=1}^3 \frac{p_{a,i}^2}{2m}, \quad (1)$$

where $p_{a,i}$ and $x_{a,i}$ are the momentums and coordinates of atoms, respectively, K is the kinetic energy, m and N are the mass and number of atoms, and U and V_{ext} are the potentials of interatomic interaction and external forcing, respectively, subscript a denotes the number of the atom, and i is the number of the coordinate. The potential of interatomic interaction U was chosen to be the Jonson multiparticle potential [5] calculated by the embedded atom method:

$$U = \sum_{a=1}^N F(\rho_a) + \frac{1}{2} \sum_{a=1}^N \sum_{b \neq a}^N \varphi(r_{ab}), \quad \rho_a = \sum_{b \neq a}^N f(r_{ab}). \quad (2)$$

Khristianovich Institute of Theoretical and Applied Mechanics, Siberian Division, Russian Academy of Sciences, Novosibirsk 630090; kiselev@itam.nsc.ru. Translated from *Prikladnaya Mekhanika i Tekhnicheskaya Fizika*, Vol. 48, No. 3, pp. 133–141, May–June, 2007. Original article submitted November 1, 2006.

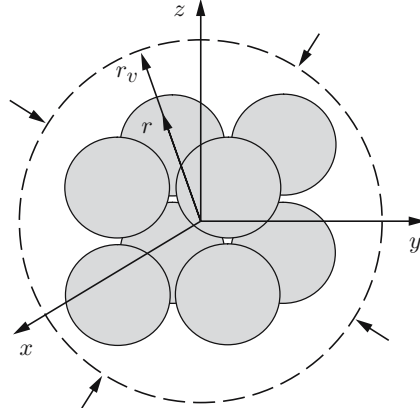


Fig. 1. Scheme of copper nanocell loading by a spherical piston.

Here ρ_a is the electron density at the point where the atom a is located and r_{ab} is the distance between the atoms a and b . The first term in the right side of the first equation in (2) describes attraction of atoms due to interaction with the electron gas, and the second term describes repulsion of positively charged atoms due to the Coulomb interaction. The second equation in (2) describes the electron density in the atom a generated by all other atoms. The analytical expressions for the functions F , φ , and f were given in [5]. Note that the Jonson potential (2) was used in [6] to calculate the deformation of a copper nanocrystal under uniaxial extension and in [7] to calculate the impact of a spherical copper particle on a rigid target. The nanocell was loaded by a spherical piston (see Fig. 1). Piston interaction with atoms was modeled by an external potential chosen in the form of a certain part (corresponding to the repulsion force) of the Lennard-Jones potential. The piston acts on the atoms located in a thin layer near the piston surface with a force $\tilde{F}_{a,i}$ directed toward the cell center:

$$\tilde{F}_{a,i} = -\frac{\partial V_{\text{ext}}(r)}{\partial x_{a,i}}, \quad V_{\text{ext}}(r) = A \left(\frac{r_0}{r - r_v} \right)^{12}, \quad r = \sqrt{(x_a^1)^2 + (x_a^2)^2 + (x_a^3)^2}. \quad (3)$$

Here the piston radius r_v is a prescribed function of time t (see Fig. 1).

The system of ordinary differential equations (1) with potentials (2) and (3) was solved numerically by the Verlet scheme [4]. A cut-off radius r_c was introduced to speed up the computations, and the computational domain was divided into cubic cells for which ‘‘coupled lists’’ were composed [4]. The computations included only those atoms that were within a distance $r_{ab} < r_c$ ($r_{ab} = \sqrt{(x_a^1 - x_b^1)^2 + (x_a^2 - x_b^2)^2 + (x_a^3 - x_b^3)^2}$). In this case, if an atom crosses the boundary of a sphere of radius r_c , there arise jumps of force and energy. To eliminate these jumps, the functions $f(r)$ and $\varphi(r)$ in (2) were replaced by the functions [4]

$$\tilde{f}(r) = \begin{cases} f(r) - f(r_c) - (df/dr)|_{r_c} (r - r_c), & r < r_c, \\ 0, & r \geq r_c, \end{cases}$$

$$\tilde{\varphi}(r) = \begin{cases} \varphi(r) - \varphi(r_c) - (d\varphi/dr)|_{r_c} (r - r_c), & r < r_c, \\ 0, & r \geq r_c. \end{cases}$$

The solutions of Eqs. (1) were the momentums and coordinates of atoms, which were further used to find the mean pressure P and temperature T in the nanocell [4]:

$$P = nkT + \frac{1}{3V} \sum_{a=1}^N \sum_{i=1}^3 F_a^i x_a^i, \quad F_a^i = \sum_{b \neq a}^N F_{ab}^i, \quad x_{ab}^i = x_a^i - x_b^i,$$

$$F_{ab}^i = -\frac{\partial U}{\partial x_{ab}^i}, \quad p_{a,i} = mv_{a,i}, \quad \langle v_{a,i} \rangle = \frac{1}{N} \sum_{a=1}^N v_{a,i},$$

$$T = \frac{2}{3Nk} \sum_{a=1}^N \sum_{i=1}^3 \frac{mv'_{a,i}v'_{a,i}}{2}, \quad v'_{a,i} = v_{a,i} - \langle v_{a,i} \rangle.$$

Here k is the Boltzmann constant and V is the volume occupied by atoms.

Before loading, the nanocell was “cooled” to a temperature of 0.014 K by solving modified Eqs. (1) with an added viscous friction force $F_v^i = -\xi v_{a,i}$ [6]. The cluster was “cooled” by calculating the coordinates and momentums of copper atoms at the moment the piston was at rest (the size of the “cooled” nanocell was $l = 2.4$ nm, the nanoparticle radius was $R_p = 0.5$ nm, and the number of copper atoms was $N = 640$). The values of the parameters involved into potential (2) were given in [5], and the cut-off radius was $r_c = 5.82$ Å. The following measurement units were used in numerical calculations: 1 g for mass, 1 Å = 10^{-10} m for length, and 1 fsec = 10^{-15} sec for time.

The nanocell was loaded by means of compression and expansion of the spherical piston. At the beginning (at the time $0 < t < t_1$), the piston was compressed with a constant acceleration v_0/t_0 . The piston radius during this period was determined by the equation $r_v(t) = r_v^0 - v_0 t^2 / (2t_0)$. Then ($t_1 < t < t_2$), the piston was decelerated and expanded with an acceleration v_0/t_3 . In this case, the piston radius was found from the equation $r_v(t) = r_v(t_1) + dr_v(t_1)/dt + v_0(t-t_1)^2 / (2t_3)$. The calculations were performed with the following values of parameters in potential (3) and piston acceleration: $A = 3 \cdot 10^{-21}$ J, $r_0 = 2$ Å, $r_v^0 = 1.8$ nm, $v_0 = 37$ m/sec, $t_0 = 1.9 \cdot 10^{-11}$ sec, and $t_3 = 10^{-11}$ sec. In this case, the strain rate of the nanocell $\dot{\epsilon}$ was of the order of $v_0 / (2R_p) \approx 4 \cdot 10^{10}$ sec $^{-1}$.

Discussion of Numerical Results. Figure 2 shows a nanocell consisting of copper atoms, being compressed by a spherical piston (side view). The calculated mean parameters are shown in Fig. 3 as functions of the time t . The true density of copper is $\rho_s = Nm/V$ (V is the volume occupied by copper atoms). The mean density of the nanocell material was determined by the formula $\rho = Nm / (V + 4V_{\text{void}})$, where V_{void} is the volume of the void in the center of the cell. (The factor 4 at the void volume V_{void} appears because each boundary of the nanocell initially corresponds to one half of the void volume V_{void} .)

It is seen in Figs. 2 and 3 that elastic oscillations of the nanocell occur first, which leads to oscillations of the mean parameters. Then, at $t > 5 \cdot 10^3$ fsec, the void filling begins (see Fig. 2b), accompanied by release of significant thermal energy and nanocell heating (see Fig. 3b). The atomic structure of the nanocell becomes amorphous. Owing to the thermal motion of molecules, the pressure, density, and temperature (see Fig. 3) start to rapidly oscillate around the mean values, which change slowly during compression and expansion of the nanocell. Temperature fluctuations and non-central interactions of atoms make the spatial distribution of atoms deviate from the spherically symmetric distribution (see Fig. 2b). Plastic filling of voids leads to irreversible growth of the mean density and temperature, while the true density ρ_s decreases, which is caused by thermal expansion of the material.

The behavior of the mean parameters in the nanocell seems to be unusual (see Fig. 3). A drastic increase in the mean density (see Fig. 3c) indicates that the voids are already filled by the time $t \approx 10^4$ fsec; therefore, the mean pressure in the nanocell is expected to increase under the further compression of the piston. As is shown in Fig. 3a, however, it remains equal to zero until $t \approx 2 \cdot 10^4$ fsec. This effect is caused by instability of the nanocell considered. A small perturbation generated by piston motion leads to void filling under the action of surface tension during the time $\Delta t \approx 2 \cdot 10^3$ fsec. During this time, the nanocell surface is shifted by a distance of the order of 2 Å, and the piston is shifted by a distance $\Delta r_v \approx v_0 \Delta t / 2 \approx 0.18$ Å. As a result, the nanocell is separated from the piston, and the mean pressure in the nanocell remains equal to zero until the piston reaches the nanocell surface at the time $t \approx 2 \cdot 10^4$ fsec. Separation of atoms from the piston is also responsible for the singularity in the dependence of energy on time, which is plotted in Fig. 3e. At $t \approx 10^4$ fsec, the kinetic (thermal) energy of the nanocell increases owing to a decrease in the potential energy of interatomic interaction that occurs during void filling. At the same time, the total energy remains constant ($\Delta E = K + \Delta U = 0$) until $t \approx 2 \cdot 10^4$ fsec. When the piston reaches the nanocell surface, the total energy E increases at the expense of the piston work during its compression, and then E decreases during piston expansion.

To check the assumption on copper nanocell instability, we calculated a situation without the spherical piston, where the initial perturbation was generated by “heating” the nanocell to a temperature of the order of 3 K. In this case, spontaneous filling of voids in the nanocell due to surface tension occurred. The time-dependent behavior of the mean parameters was the same as that in Fig. 3 in the time interval from $t = 0$ to $t \approx 2 \cdot 10^4$ fsec.

Let us estimate the increase in temperature and the characteristic time of pore filling. The total area of the free surface of nanoparticles is $S_1 \approx 4\pi \cdot 8 \cdot 0.5^2$ nm 2 at the initial time and $S_2 \approx 4\pi \cdot 1$ nm 2 after void filling. Using $\alpha_\sigma \approx 0.5$ J/m as an estimate of the surface energy, we find the change in the surface energy of the nanocell due to

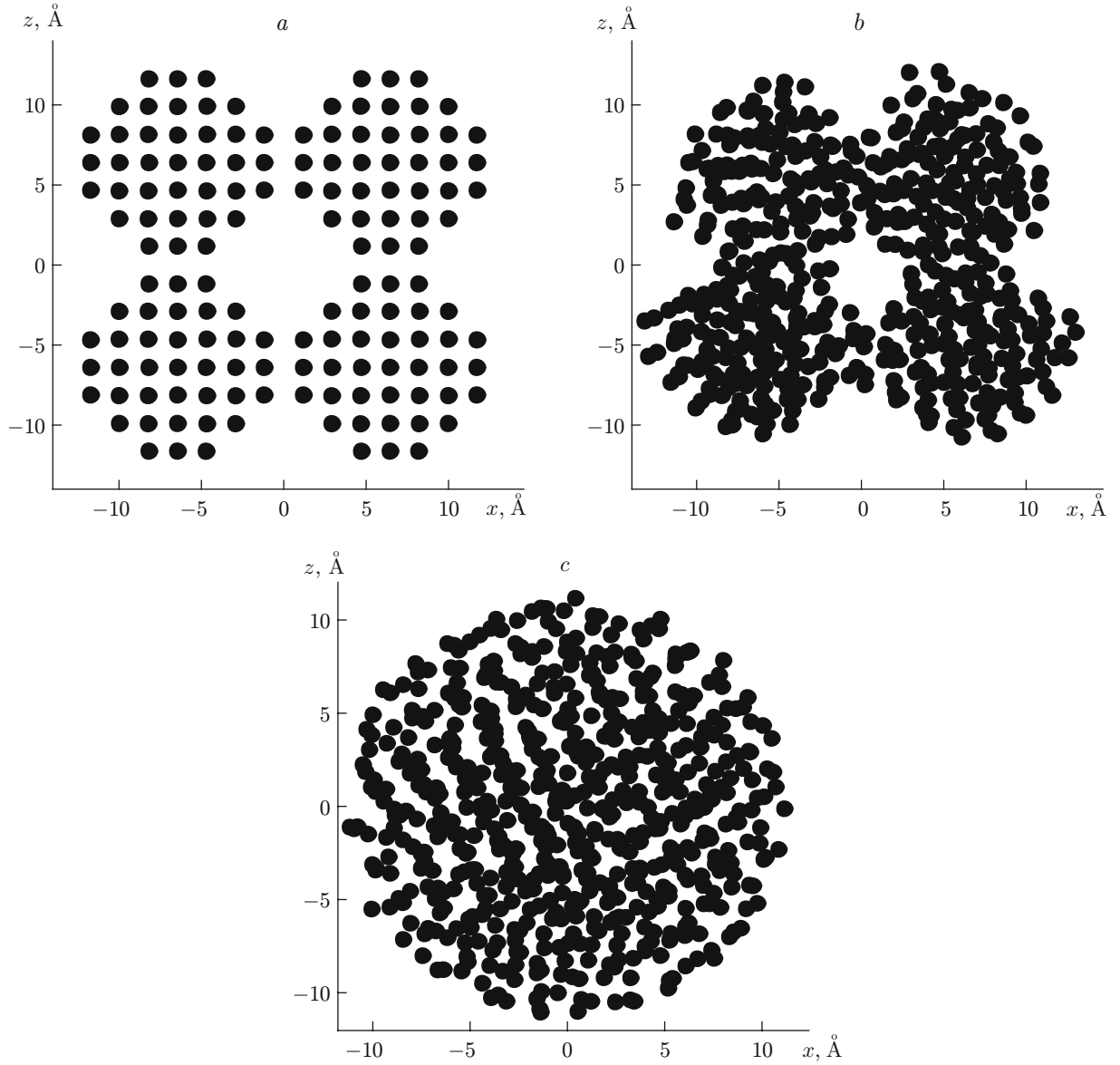


Fig. 2. Positions of nanocell atoms in the plane (x, z) under compression by a piston ($v_0 = 37$ m/sec) at different times: $t = 2.5 \cdot 10^3$ (a), $7.5 \cdot 10^3$ (b), and $2.5 \cdot 10^4$ fsec (c).

void filling: $\Delta E_\sigma \approx \alpha_\sigma(S_1 - S_2) \approx 6.2 \cdot 10^{-18}$ J. Using the results in Fig. 3b, we find the change in the nanocell temperature ($\Delta T \approx 500$ K) and the increment of the thermal energy [$K = (3/2)Nk\Delta T \approx 6.5 \cdot 10^{-18}$ J]. Hence, it follows that nanocell heating occurs owing to a decrease in surface energy: $K \approx \Delta E_\sigma$.

Using the Π -theorem, we estimate the characteristic time of void filling: $\tau_\alpha \approx R_p^{3/2} / \sqrt{2\alpha_\sigma/\rho_s} \approx 10^{-12}$ sec. This estimate is close to the time of void filling obtained in numerical calculations: $\Delta t \approx 2 \cdot 10^{-12}$ sec. Note that similar features (heating of nanoparticles and pressure oscillations) are also observed in coagulation of carbon nanoparticles, which were considered in a two-dimensional formulation by the method of molecular dynamics in [8]. (The interaction of carbon atoms was described in [8] by the Lennard-Jones potential.)

If the velocity of piston compression is increased by an order of magnitude, no separation of the nanocell from the piston occurs if the following inequality holds: $\dot{\epsilon} \approx v_0/(2R_p) > 1/\tau_\alpha$. Figures 4 and 5 show the calculated atomic configurations and the mean parameters for the case of compression of the nanocell by the piston with a velocity ($v_0 = 370$ m/sec) such that the strain rate of the nanocell is $\dot{\epsilon} \approx v_0/(2R_p) \approx 4 \cdot 10^{11}$ sec $^{-1}$. It is seen that the nanocell permanently experiences the influence of the spherical piston and the atomic configuration remains

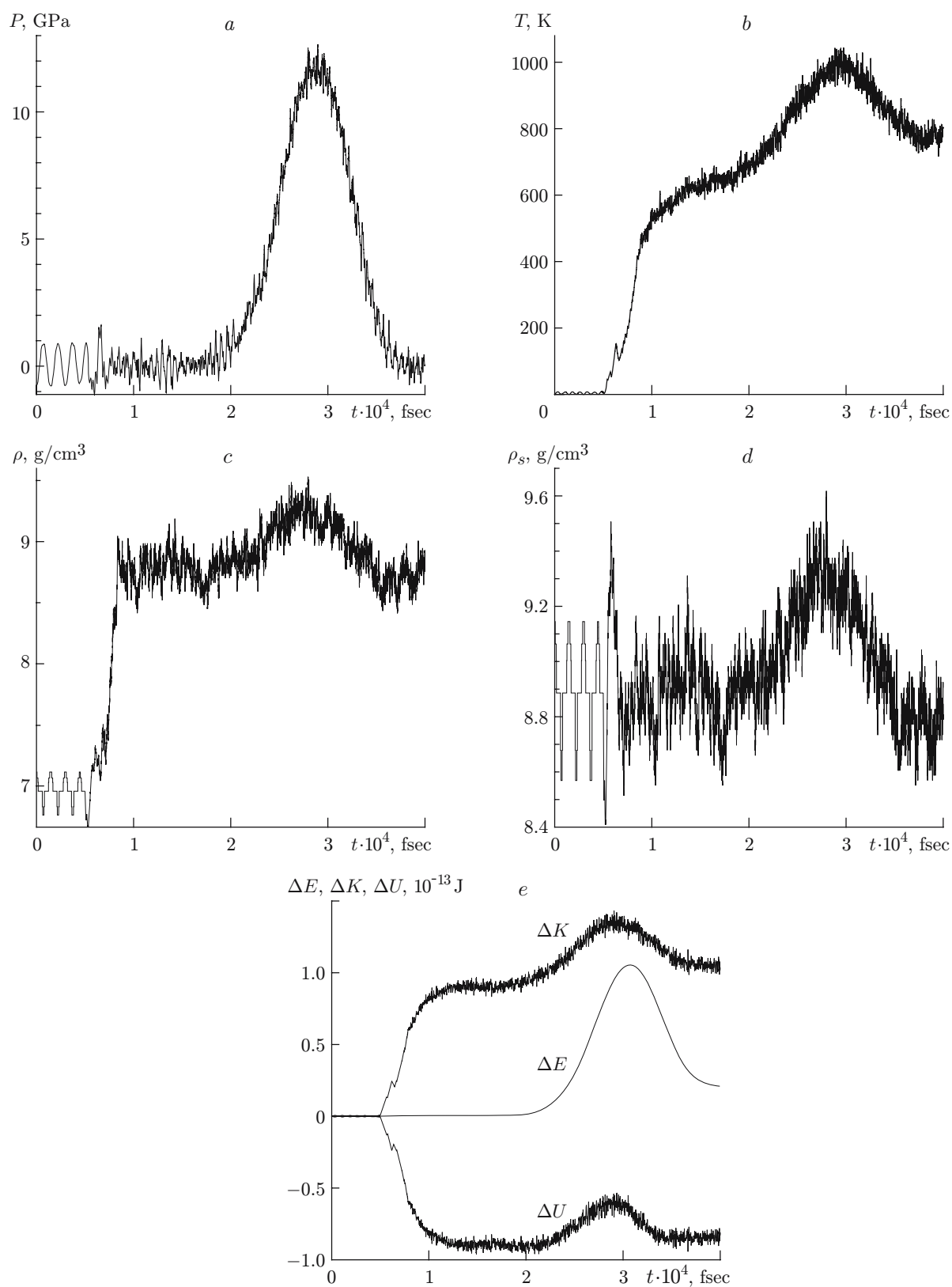


Fig. 3. Calculation of the mean parameters for a nanocell compressed by a spherical piston ($v_0 = 37$ m/sec): (a) $P(t)$; (b) $T(t)$; (c) $\rho(t)$; (d) $\rho_s(t)$; (e) $\Delta E = E(t) - E|_{t=0}$, $\Delta K(t) = K(t)$, and $\Delta U = U(t) - U|_{t=0}$.

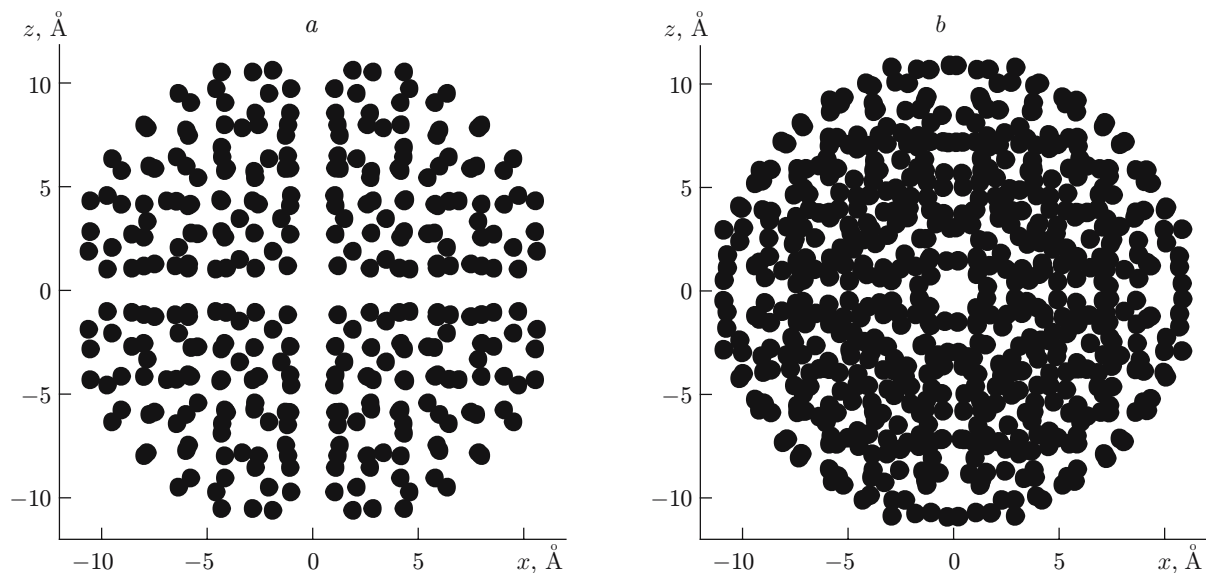


Fig. 4. Positions of nanocell atoms in the plane (x, z) under compression by a piston ($v_0 = 370$ m/sec) for $t = 2.4 \cdot 10^3$ (a) and $2.8 \cdot 10^3$ fsec (b).

symmetric. The pressure, density, temperature, and energy of the nanocell increase under piston compression and decrease under piston expansion (see Fig. 5). Oscillations with a period of 600 fsec are superimposed on the dependences of the mean parameters on time; these oscillations are caused by propagation of compression and expansion waves in the nanocell with a characteristic time $\tau \approx R_p/c \approx 500$ fsec ($c \approx 4 \cdot 10^3$ m/sec is the volume velocity of sound in copper). Piston compression leads to an increase in the total, kinetic, and potential energy (see Fig. 5f). The potential energy increases faster than the kinetic energy until $t \approx 2.8 \cdot 10^3$ fsec when a drastic increase in the kinetic energy occurs owing to a decrease in the potential energy. Figure 5a shows the function of the radial distribution of atomic density $g(r) = (dN(r)/dr)/(4\pi r^2 N n)$ [r is the distance between the atoms and $dN(r)$ is the number of atoms in a spherical layer $(r, r + dr)$] for two times. It is seen that the function $g(r)$ corresponds to a strongly distorted crystalline structure at the time $t = 2.4 \cdot 10^3$ fsec and to an amorphous structure at the time $t = 2.8 \cdot 10^3$ fsec. Hence, we can conclude that a phase transition with a significant heat release occurs at the time $t \approx 2.8 \cdot 10^3$ fsec. The translation order disappears, and the nanocell passes to an amorphous state.

The emergence of the phase transition in the system is caused by a high rate of loading of the nanocell. The atoms in the crystal occupy the states determined by interaction with the moving piston. These states, however, are not equilibrium and energetically beneficial; therefore, the potential energy increases much faster than the kinetic energy until the phase transition. At a temperature of 1800 K (see Fig. 5c), the atomic system relaxes and passes to a more stable state with a lower potential energy. Then this state tends to equilibrium, which is manifested in equal values of the potential and kinetic energies at $t > 4 \cdot 10^3$ fsec.

Conclusions. The calculations performed showed that the copper nanocell is an unstable system. Small perturbations generated by piston motion (with a piston velocity of the order of 37 m/sec) lead to spontaneous filling of voids under the action of the surface tension force. A significant amount of the thermal energy is released thereby, leading to nanocell heating to a temperature of the order of 500 K. Owing to void filling, the original crystalline structure of nanoparticles is violated, and the nanoparticle acquires an amorphous structure. If the nanocell is compressed with a high velocity (with a piston velocity of the order of 370 m/sec), the governing effect on the nanocell structure is exerted by the piston. In the course of compression, there arises a metastable state with a strongly distorted crystal lattice. As the temperature reaches a critical value equal to 1800 K, a phase transition occurs, and the metastable state transforms to an amorphous state with a significant heat release.

This work was supported by the Russian Foundation for Basic Research (Grant No. 04-01-00894-a), by the Integration Project No. 106 of the Siberian Division of the Russian Academy of Sciences, and Foundation “Leading Scientific Schools of Russian Federation” (Grant No. NSh-9019.2006.1).

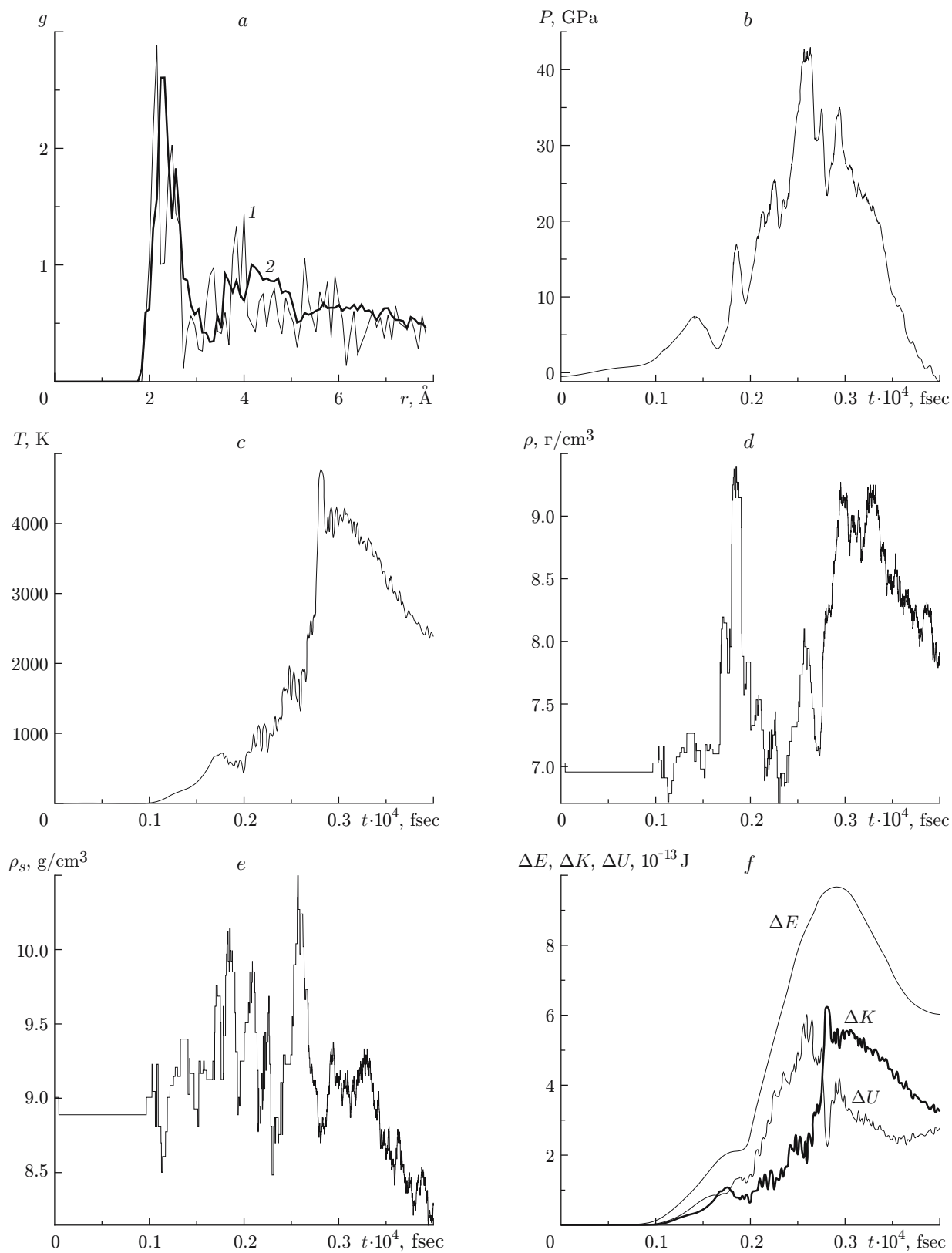


Fig. 5. Calculation of the mean parameters for a nanocell compressed by a spherical piston ($v_0 = 370$ m/sec): (a) $g(r)$; curve 1 refers to $t = 2.4 \cdot 10^3$ (before the phase transition) and curve 2 refers to $t = 2.8 \cdot 10^3$ fsec (after the phase transition); (b) $P(t)$; (c) $T(t)$; (d) $\rho(t)$; (e) $\rho_s(t)$; (f) $\Delta E(t)$, $\Delta K(t)$, and $\Delta U(t)$.

REFERENCES

1. S. V. Klinkov and V. F. Kosarev, "Measurements of cold spray deposition efficiency," *J. Thermal Spray Technol.*, **15**, No. 3, 364–371 (2006).
2. V. V. Ivanov, Yu. A. Kotov, A. N. Vikhrev, and N. I. Noskova, "Hot dynamic compaction of nanosize powders of aluminum and titanium oxides," *Dokl. Ross. Akad. Nauk*, **352**, No. 6, 759–761 (1997).
3. D. V. Dudina, O. I. Lomovsky, M. A. Korchagin, and V. I. Mali, "Reactions in the metallic matrix: Synthesis and properties of TiB₂–Cu nanocomposites," *Khim. Inter. Ustoich. Razv.*, **12**, No. 3, 319–325 (2004).
4. M. P. Allen and D. J. Tildesley, *Computer Simulation of Liquids*, Oxford University Press, Oxford (1987).
5. R. A. Jonson, "Alloy models with the embedded-atom method," *Phys. Rev. B*, **39**, 12554–12559 (1989).
6. E. I. Golovneva, I. F. Golovnev, and V. M. Fomin, "Modeling of quasi-static processes in crystals by the method of molecular dynamics," *Fiz. Mezomekh.*, **6**, No. 6, 5–10 (2003).
7. A. V. Bolesta, I. F. Golovnev, and V. M. Fomin, "Studying the impact of a spherical cluster of copper on a rigid wall by the method of molecular dynamics," *Fiz. Mezomekh.*, **3**, No. 5, 39–46 (2000).
8. A. L. Kupershtokh, A. P. Ershov, and D. A. Medvedev, "Model for the coagulation of carbon clusters at high densities and temperatures," *Combust., Expl., Shock Waves*, **34**, No. 4, 460–466 (1998).